IONOSPHERIC DELAYS COMPENSATION FOR ON-THE-FLY INTEGER AMBIGUITY RESOLUTION IN LONG BASELINE LEO FORMATIONS

PAPER PUBLISHED AS:

Tancredi, U.; Renga, A. & Grassi, M. (2014), 'Ionospheric Delays Compensation for On-The-Fly Integer Ambiguity Resolution in Long Baseline LEO Formations', International Journal of Space Science and Engineering 2, 63-80.

DOI 10.1504/IJSPACESE.2014.060107

IONOSPHERIC DELAYS COMPENSATION FOR ON-THE-FLY INTEGER AMBIGUITY RESOLUTION IN LONG BASELINE LEO FORMATIONS

Urbano Tancredi [(1)]**, Alfredo Renga**[(2)]**, and Michele Grassi**[(3)]
[(1)]*Department of Engineering, University of Naples Parthenope, Centro Direzionale C4, Napoli, 80143, Italy, +390815476744, urbano.tancredi@uniparthenope.it*
[(2)]*Department of Industrial Engineering, University of Naples Federico II, Piazzale Tecchio 80, Napoli, 80125, Italy, alfredo.renga@unina.it*
[(2)]*Department of Industrial Engineering, University of Naples Federico II, Piazzale Tecchio 80, Napoli, 80125, Italy, michele.grassi@unina.it*

Abstract:This paper deals with the real-time onboard accurate relative positioning by Carrier-phase Differential GPS (CDGPS) of LEO formations with baselines of hundreds of kilometers. On long baselines, high accuracy can be achieved only using dual-frequency measurements and exploiting the integer nature of Double Difference (DD) carrier-phase ambiguities. However, large differential ionospheric delays and broadcast ephemeris errors complicate the integer resolution task. The present paper is concerned with analyzing possible approaches to DD ionospheric delays compensation in such applications. Two different strategies are implemented to deal with DD ionospheric delays. The first formulation models differential ionospheric delays as a function of the vertical total electron content above the receivers, whereas the second one is based on combining the DD measurements for removing ionospheric delays from the observation model. The effectiveness of the developed solutions is assessed by comparing the relative positioning accuracy that can be obtained on actual flight data from the Gravity Recovery and Climate Experiment mission. This is done using a recently developed, common relative positioning approach. Results show that ionospheric activity plays a major role in determining the relative positioning performance. Modeling the delays is advantageous for relative positioning in mild ionospheric conditions, but the solution without ionospheric delays becomes preferable as the ionosphere's electron content increases.

Keywords: LEO formations, Precise Relative Positioning, Long Baseline, Carrier-phase Differential GPS, On-the-fly Integer Ambiguity Resolution, Ionospheric Delays.

Biographical notes:

Urbano Tancredi is an assistant professor of aerospace systems in the Department for Technologies at the University of Naples Parthenope since 2008. He received in 2005 a Ph.D. in aerospace sciences and technologies from the Second University of Naples. His research interests are in the areas of guidance, navigation, and control of aerospace systems, and air traffic management.

Alfredo Renga received the M.S. degree (2006) and the Ph. D. degree (2010) in Aerospace Engineering at the University of Naples "Federico II" (UniNa). He's currently a post-doc researcher at the Department of Industrial Engineering of UniNA. Dr. Renga has developed his research activity within two main topics: (1) Remote Sensing and Surveillance Applications by Synthetic Aperture Radar, (2) Relative Navigation by GPS.

Michele Grassi was born in Naples in 1963. Since 1998 He has been associate professor of Space Systems at the Department of Industrial Engineering - Aerospace Section - of University of Naples “Federico II”, Naples, Italy. His research field covers the guidance, navigation, and control of aerospace systems and the space system design. He has been principal investigator and co-investigator in national and international projects on the topic, and chair/co-chair in national and international conferences. His research results have been published in distinguished international journals.

1 Introduction

This paper analyzes the problem of real-time onboard precise relative positioning of long-baseline LEO formations by Carrier-phase Differential GPS (CDGPS). Herein long-baseline is intended as satellite separations in the order of hundreds of kilometers and precise denotes centimeter/decimeter level positioning accuracy.
When dealing with LEO formations with large separations, dual-frequency Carrier-phase differential GPS (CDGPS) is the most promising solution for precise relative navigation [1]. Indeed, exploiting the integer nature of Double Difference (DD) carrier-phase observables allows, in principle, determining the baseline with high accuracy, up to the millimeter/centimeter level. However, in long baseline applications differential ionospheric delays and broadcast ephemeris errors affect DD GPS measurements significantly and complicate the integer resolution task [2]. These, can easily spoil accuracy and robustness of the integer ambiguities (IA) solution, seriously degrading the baseline estimate.
In particular, both DD ephemeris and ionospheric error increase with the baseline. For baselines in the order of hundreds of kilometers, such as those of interest for this paper, these two errors cannot be neglected for precise relative positioning. DD broadcast ephemeris cause errors on the measured DD ranges in the order of 5 cm for the baseline of interest. The magnitude of DD ionospheric delays can be substantially higher, also depending on the ionosphere’s electron content. The electron content varies sensibly depending on multiple factors, most notably the 11-year long solar activity cycle. As a result, the difference between the ionospheric delays under mild and severe ionospheric activity can exceed one order of magnitude. Thus, the relative positioning accuracy on long baseline applications can heavily depend on the ionospheric activity.
The open literature proposes many works dealing with CDGPS-based relative navigation of LEO formations, however the most part describes approaches suitable for short-baseline applications (i.e. up to tens of kilometers) [3]–[6], in which DD ionospheric delays need not to be explicitly compensated. Only few authors investigate approaches for precise relative positioning of satellites separated hundreds of kilometers, even though for post-processing reconstruction of the relative orbit [1], or real-time relative positioning but using precise ephemeris products [7]. These works demonstrate that sub-centimeter relative positioning accuracy on flight data can be achieved with closed-loop approaches in which all the fixed integer ambiguities are fed back to improve the float estimate provided by an Extended Kalman Filter (EKF). In these approaches, highly complex models of the satellites’ orbital dynamics support the ambiguity resolution task. These approaches can be not suitable for real-time onboard applications. First, the dynamic models’ complexity should be reduced, which worsens the relative positioning accuracy of at least an order

of magnitude [4]. The higher residual error of using broadcast ephemeris shall also be accounted for.
Accounting for DD ionospheric delays in LEO relative positioning has also been done in multiple ways. For baselines smaller than 10 km they are generally ignored [4]. In high accuracy applications with dual frequency data (e.g. [1],[3],[7]) , differential ionospheric delays are estimated along with the other unknowns using random walk models. In single-frequency applications with demanding accuracy requirements, such as [3],[5],[6], the ionospheric delays are approximated assuming a unique common Vertical Total Electron Content (VTEC) using a simplified model introduced by Lear [8]. Lear's model has also been used with dual frequency data and assuming a variable VTEC along the baseline for improving its prediction accuracy [2],[9],[10].
The present paper is concerned with analyzing potential solutions towards real-time onboard CDGPS (Carrier-phase Differential GPS), by evaluating their relative positioning performance on GRACE (Gravity Recovery and Climate Experiment) data, taking into account different ionospheric activity levels. Possible approaches to DD ionospheric delays compensation are reviewed, and two different strategies are implemented. In one approach ionospheric delays are specifically modeled in the filter assuming a variable VTEC along the baseline, whereas in the other approach the ionosphere's first-order effect is removed by suitable combinations of dual-frequency DD measurements. The effectiveness of these two approaches in compensating ionospheric delays is then evaluated by comparing their relative positioning accuracy that can be obtained on actual flight data. This is done using a recently developed common relative positioning approach [11], which is described next.

2 Refererence relative positioning scheme

A closed-loop scheme for integrating an EKF and an integer resolution approach has been proposed in [11] and it is considered herein as a reference solution for real-time onboard CDGPS in long baseline applications. The main features of this reference scheme are briefly recalled in the following, and the interested reader is referred to [11] for further details.
The proposed approach, conceptually sketched in Figure 1, consists in a two-step solution: first DD integer ambiguities are estimated On-The-Fly (OTF) using as little computational effort as possible. Then, the second step provides the relative position with high accuracy using the fixed integer ambiguities to obtain a Real-Time Kinematic (RTK) solution. Because of this architecture, a precise relative position can be obtained only relying on the fixed integer ambiguities. As long as the ambiguities are correctly fixed, this allows using low fidelity models in the first step without affecting the relative position accuracy, with related computational benefits.
The structure of the OTF ambiguity resolution is shown in Figure 2. In this mixed integer continuous dynamical filter an EKF is in charge of generating the float estimate, that is, the estimation of all the variables as real-valued, integer ambiguities included. The EKF state vector comprises the relative position and velocity and the Wide-Lane (WL) and L1 cycle ambiguities. Depending on the ionospheric delay compensation strategy, additional terms might be added to the state vector.

With specific reference to a formation of two satellites, named chief and deputy, the relative dynamics are modeled by a nonlinear Keplerian relative orbital motion augmented with J2 effects and with additive process noise $\mathbf{v}_b$.

$$\ddot{\mathbf{b}} = \frac{\mu}{r_C^3}\left[C_1\left(r_\oplus, J_2, \mathbf{r}_C\right)\cdot\mathbf{r}_C + C_2\left(r_\oplus, J_2, \mathbf{r}_C, \mathbf{b}\right)\cdot\left(\mathbf{r}_C+\mathbf{b}\right)\right] + \boldsymbol{\Omega}_\mathbf{E}\times\boldsymbol{\Omega}_\mathbf{E}\times\mathbf{b} + 2\boldsymbol{\Omega}_\mathbf{E}\times\dot{\mathbf{b}} + \mathbf{v}_b \quad (1a)$$

$$C_1\left(r_\oplus, J_2, \mathbf{r}_C\right) = 1 + \frac{3}{2}\frac{J_2 r_\oplus^2}{r_C^2} - \frac{15}{2}\frac{J_2 r_\oplus^2}{r_C^4} r_z^2 \quad (1b)$$

$$C_2\left(r_\oplus, J_2, \mathbf{r}_C, \mathbf{b}\right) = -\frac{r_C^3}{\sqrt{\left(r_c^2 + 2\left\langle \mathbf{r}_C, \mathbf{b}\right\rangle + b^2\right)^3}} C_1\left(r_\oplus, J_2, \mathbf{r}_C + \mathbf{b}\right) \quad (1c)$$

where **b** is the baseline between the receivers, μ is the Earth gravitational constant, $r_\oplus$ is the Earth equatorial radius, J_2 is the second zonal harmonic, $\boldsymbol{\Omega}_E$ is the Earth angular velocity vector in ECEF, r_z is the ECEF component of chief position vector $\mathbf{r}_c$ along z-axis, $\langle\cdot,\cdot\rangle$ indicates the scalar product, and × represents the vector product. The Jacobian of the considered dynamics model is not reported for the sake of brevity, but it can be computed analytically after trivial algebra.The selected dynamics are a trade-off between complex but accurate trajectory propagation and a computational load adequate for real-time on board implementation. The above model, being concerned with relative dynamics, allows modeling differential perturbations (e.g. differential drag) as process noise while keeping low the computational effort [12]. The same model, i.e. non linear Keplerian relative model augmented with J_2 effects, is assumed also for the absolute dynamic of the chief satellite. As a consequence, Eq.(1) are propagated together with the chief absolute dynamics, resulting in a total of six second-order, nonlinear, ordinary differential equations (ODE). Solution of the ODE system is achieved using a 4th order Runge-Kutta integration method. After the solution is computed, only *b* and $\dot{b}$ are retained in the filter's state vector, whereas absolute chief dynamics are not maintained, but computed at each time epoch by standard kinematic techniques.

Starting from the float estimate, the Least-squares AMbiguity Decorrelation Adjustment (LAMBDA) method [13] is used to conduct the integer searching step. The integer nature of the validated ambiguities is then exploited to correct the real-valued float estimate, yielding the fixed estimate. This is fed back to the EKF to improve the solution in the following time instants. However, in presence of errors in the estimated IA, the fixed solution can be less accurate than the float one. Establishing the conditions in which the IA vector is suitable for being fixed or not is a non trivial task. The fixed solution is usually computed only when the IA vector can be assumed to be correct with a certain confidence level. Several integer validation tests have been designed for this purpose and are customarily employed in relative positioning by CDGPS. A thorough discussion of this topic is available in [14], which also proposes novel validation tests that take explicitly into account the probability distribution of LAMBDA's integer estimates. Basically, the Integer Least Squares (ILS) estimation theory assumes that the float ambiguities estimates are de-biased and affected by a Gaussian error. When the float estimate probability distribution is sufficiently sharp to allow neglecting the stochastic nature of the LAMBDA integer estimates, these can be used to improve the float solution and yield the fixed solution [14]:

$$\breve{\boldsymbol{\beta}} = \hat{\boldsymbol{\beta}} + P_{\beta\alpha}P_{\alpha\alpha}^{-1}\left(\breve{\boldsymbol{\alpha}} - \hat{\boldsymbol{\alpha}}\right) \;;\; P_{\beta|\breve{\alpha}} = P_{\beta\beta} - P_{\beta\alpha}P_{\alpha\alpha}^{-1}P_{\alpha\beta} \quad (2)$$

where the baseline vector **β** comprises all the state vector components but the validated ambiguities (both WL and L1) that are included in the vector **α**. The symbols ˆ and ˇ refer to the float and fixed estimates, respectively, and P_{cd} stands for the float covariance matrix between the generic variables *c* and *d*.

Unfortunately, the theoretical assumptions upon which the LAMBDA method and the integer validation tests are based do not hold in real-time long-baseline applications. Both the DD broadcast ephemeris error and the residual DD ionospheric path delay are far from being unbiased and Gaussian distributed. As such, the standard IA fixing technique described above is not applicable for obtaining instantaneous integer ambiguity resolution. In order to exploit the proposed low-fidelity computationally-efficient float solution we instead rely on using as much as possible the integer ambiguity time correlation.

In fact, because the cycle ambiguities are constant in time for a specific DD couple, the fixed solution can also be fed back to the EKF for improving the float estimate at the following time instants, closing the loop between the float solution and the ILS estimator. This closed loop arrangement is used in most works concerned with high-accuracy spaceborne relative positioning [1],[5],[7]. Feedback to the EKF is given either by direct substitution of the fixed solution into the state vector, or by an additional pseudo-measurement step of the EKF (see [1], for instance), which can be proved to be equivalent to Eq.(2) by trivial algebra. The closed loop scheme is able to further sharpen the fixed ambiguities estimate about the correct integer values despite the time-correlated ephemeris and ionospheric errors, but is less robust to erroneously fixed integer ambiguities. Wrong IA will affect the filter solution in all the following time instants, spoiling the quality of the estimation of future ambiguities. This might easily result into divergence of the solution, even for very low fail rates [5], [14]. This arrangement is thus potentially capable of better IA fixing performances, but lacks in robustness when compared to the standard open-loop one.

When using the closed-loop approach, the integer validation step becomes thus of crucial importance. From the one hand, the validation test shall allow fixing the correct integer estimates as much as possible, in order to sharpen the ambiguities estimate at later time epochs. From the other hand, the validation cannot let erroneous integer ambiguities to be fixed, which would rapidly spoil the closed loop solution quality. Lacking the applicability of their basic assumptions, standard integer validation tests have already shown unsatisfactory performance in long baseline relative positioning of spaceborne receivers, even when fed with highly accurate float estimates [1]. For these reasons, they are not applicable in the present context. One of the main shortcomings of standard validation tests is that they handle the vector of ambiguities **a** as a whole. When only a few ambiguities in the vector are erroneous, a situation that might happen frequently in the application of interest, discarding the whole vector would result in a conservative choice, whereas accepting it would let some ambiguities to be erroneously fixed. None of these two outcomes is suitable for closed-loop integer ambiguities fixing. Thus, non standard integer validation tests are instead used, which screen individual ambiguities within the ambiguity vector rather than the whole vector. Indeed, when not all the integer ambiguities are correctly fixed, there is the possibility that a subset of the integer ambiguity vector is instead correct.

Partial integer ambiguity validation tests are concerned with discriminating between the single ambiguities, i.e. separating the correct from the incorrect ones within the **a** vector. These techniques have shown potential for substantially improving the integer fixing success rate in long baseline applications [9]. However, partial validation of integer estimates of an ILS estimator presents several critical aspects from a

theoretical point of view, even when assuming the ambiguity float estimates have a de-biased Gaussian pdf. Because the ILS solution is optimal in a vector sense, selecting a subset of the ambiguity vector requires re-computing the solution. Issues such as how to select the ambiguity vector subset and its cardinality remain still unresolved, and partial integer validation of ILS solutions is still an open problem [15]. Lacking a theoretical background, but thanks to the increase in IA fixing performance that can be gained, partial integer validation techniques are customarily employed in long-baseline applications, usually designing the validation tests by common sense and following empirical guidelines (see [3],[5]–[7]). Based on the above observations, the technique we propose in this paper for performing on-the-fly ambiguity resolution is to augment the float estimate of the EKF by a closed-loop integer fixing scheme, in which the LAMBDA method yields integer ambiguity candidates which are screened by a custom-developed partial integer validation test. Integer validation is performed only on the wide-lane integer ambiguities, which are explicitly maintained in the EKF state vector in place of the usual L2 ones. More precisely, WL validation is performed by applying two different tests, which involve residuals of the float wide-lane ambiguity and of the Melbourne-Wubbena (MW) measurement combinations [16].

This validation test has an intuitive theoretical justification. Partial validation of the components of the ambiguity *v*ector would be possible with no theoretical difficulties in case the screened individual ambiguities would be uncorrelated. In this trivial case, the ILS solution would coincide with the one obtained rounding each float ambiguity estimate to the nearest integer and the integer ambiguities could be screened individually. The results presented in [17] suggest that the wide-lane ambiguities estimates have almost uncorrelated variance, especially when the ionosphere error contribution is high w.r.t. code measurement noise, as in long-baseline applications. Thus, WL ambiguities can be reasonably screened individually by partial integer validation tests in such applications. Moreover, it is known that decorrelation of ambiguities can occur only accompanied by an increase in precision [17]. Estimation of wide-lane ambiguities can thus be made with an increased precision w.r.t. uncombined ambiguities, as witnessed by the numerous integer fixing approaches proposed in the open literature which are based in some way on WL combinations. Thus, our choice of the validation test allows exploiting the advantages of the closed-loop scheme, by incorporating as much correct WL ambiguities as possible into the fixed solution thanks to their correlation properties, while minimizing the fail rate thanks to the precision of WL ambiguity float estimates.

However, fixing WL ambiguities only does not allow exploiting the cm-level accuracy of the carrier phase measurements. Integer L1 ambiguity estimation must still be performed for de-biasing the ionospheric-free carrier-phase observations. The WL-closed-loop fixed solution is thus used to perform an additional ILS estimation by LAMBDA. The fixed ambiguity vector, which comprises float estimates of non-valid WL and L1 ambiguities, is fed to LAMBDA along with its estimated covariance matrix. L1 ambiguities that have a fixed WL counterpart are then kept into the ambiguity resolution output. The other L1 ambiguities would not contribute to de-biasing carrier phase measurements, and are thus not needed. Note that all L1 ambiguities are computed on a single-epoch basis. If LAMBDA fails to correctly estimate some L1 ambiguities at a certain time epoch, this does not imply that the error will propagate forward in time, as opposed to what happens to ambiguities estimated within the closed-loop scheme.

3 Ionospheric delays compensation

As previously discussed, one of the main errors to be compensated in long baseline LEO relative positioning by GPS is the DD ionospheric delay. Ionospheric delays appear in all pseudorange and carrier-phase DD observation equations. When using dual frequency measurements, as in the present context, the ionospheric delays affect all four observables. However, because of their dispersive nature, the first-order ionospheric delay effect on the four observables can be accurately estimated by knowledge only of the delay on the pseudorange measurement on the L1 frequency, which we denote by *I*. More precisely, as it is well known, two receivers and two GPS satellite vehicles (SV) are needed to form a DD observable. Denoting by the *j* superscript the SV taken as a reference for the double differencing operation, usually known as the pivot, and by the *k* superscript the other SV used for differencing, for each *jk* SV pair we have the following four observation equations:

$$\begin{aligned} P_1^{jk} &= \rho^{jk}(\mathbf{b}) + \quad I^{jk} \quad + \varepsilon_{P1}^{jk} \\ P_2^{jk} &= \rho^{jk}(\mathbf{b}) + \gamma^{-2} I^{jk} \quad + \varepsilon_{P2}^{jk} \\ L_1^{jk} &= \rho^{jk}(\mathbf{b}) - \quad I^{jk} + \lambda_1 n_1^{jk} + \varepsilon_{L1}^{jk} \\ L_2^{jk} &= \rho^{jk}(\mathbf{b}) - \gamma^{-2} I^{jk} + \lambda_2 n_2^{jk} + \varepsilon_{L2}^{jk} \end{aligned} \tag{3}$$

Where $\rho(\mathbf{b})$ denotes the DD geometric term, *P* and *L* stand for the pseudorange and carrier phase measurements, respectively, λ stands for the signal wavelength, n for the integer ambiguity, ε encloses the measurement noise and all other error terms, and the subscript denotes the GPS signal frequency, whose ratio is given by $\gamma = 60/77$. Thus, when *p* SV pairs are in common view of the two receivers, there is the need to compensate *p* DD ionospheric delays. The magnitude of the DD ionospheric delays mainly depends on the baseline's magnitude, on the receivers' orbits, and on the ionospheric activity. For receivers in polar LEO separated by few hundreds of kilometers the DD delays can be about 0.5 meters in mild ionospheric conditions [10], and can increase by more than one order of magnitude depending on the ionosphere's status [11], Thus, the ionospheric delays must not only be compensated in the applications of interest, but the effectiveness of their compensation can greatly depend on the ionospheric activity.

Several approaches exist for compensating the ionospheric delays in spaceborne applications. First, the DD ionospheric delays can be approximated by a model introduced by Lear especially for LEO applications in [8], and frequently used in single-frequency or less challenging LEO applications (e.g. [2], [3], [5], [6], [10]). As an alternative, the first order ionospheric delays might be deleted exactly from the observation equations by proper linear combinations of dual frequency data. This approach is customarily used in RTK applications for ground-based dual frequency receivers. At last, differential ionospheric delays can be estimated along with the other unknowns using simple stochastic models (e.g. random walk or low order Gauss-Markov processes). This solution is frequently applied in high accuracy LEO applications with dual frequency data (e.g. [1], [3], [7]).

Each of these approaches has its own advantages and limitations. Deleting the ionospheric delays from the observation equations has the advantage of removing the

first order ionospheric delay exactly, but reduces the number of independent observations thus reducing observability of the unknowns. Estimating the individual DD delays does not change the measurements, but the unknowns increase by the number of DD pairs *p*. Because of the simple stochastic models typically used, the time correlation that can be exploited to ease the estimation of the DD ionospheric delays is typically low. As a result, this approach tends to be very similar to the former, and is not further considered in this work, At last, using Lear's model has the advantage of requiring only a very small number of additional unknowns without reducing the number of observations. In fact, Lear's model maps the vertical TEC of the receiver *A* into the L1 ionospheric delays along the ray path coming from the SV *k*, as follows.

$$I_{rec}^{sv} = m_{rec}^{sv} \cdot VTEC_{rec} \ , \ m_{rec}^{sv} = \frac{40.3}{f_1^2} \cdot \frac{2.037}{\sin\left(E_{rec}^{sv}\right) + \sqrt{\sin^2\left(E_{rec}^{sv}\right) + 0.076}} \tag{4}$$

Where the L1 frequency f_1 shall be expressed in Hz, the unit of measurement of m_{rec}^{sv} is m^3/(number of electrons), and the mapping function depends on the elevation angle of *sv* with respect to *rec*, denoted by E_{rec}^{sv}. This model has the advantage that requires estimating only the VTEC above the two receivers to estimate the *p* DD ionospheric delays. This allows, in principle, to increase the observability of the other unknowns w.r.t. the other approaches. However, the downside of using Lear's model is that it introduces a residual error because of its limited accuracy.
Thus, we will evauate the effectiveness of these two approaches in compensating the DD ionospheric delays by analyzing their performances when using the relative positioning algorithm described in section 2. The following subsections focus on the details of these two alternative closed-loop EKF schemes.

3.1 Wide-lane closed-loop EKF with Lear's model

Lear's model can be used in several ways for compensating the DD ionospheric delays. In applications with shorter baselines, a unique VTEC value common to both receivers is frequently used ([3], [5], [6]). As proposed by previous works on long baseline relative positioning scenarios ([2], [9]-[12]), we let the VTEC vary between the receivers, and thus have two potentially distinct values. The EKF state vector of this first solution is

$$x \in \mathbb{R}^{(8+2p)\times 1} \ , \ x = \left(\mathbf{b}'^{T} \quad \mathbf{VTEC}^{T} \quad \mathbf{a}_w^{T} \quad \mathbf{a}_1^{T}\right)^{T} \tag{5}$$

where **b***'* includes the relative position vector, computed from the chief to the deputy, and the relative velocity vector in ECEF (Earth Centred Earth Fixed) reference frame, **VTEC** is the vector comprising the two vertical total electron contents above the receivers, $\mathbf{a}_w$ and $\mathbf{a}_1$ represent the vector of wide-lane and L1 DD ambiguities, respectively. The corresponding EKF measurement vector is

$$y \in \mathbb{R}^{4p\times 1} \ , \ y = \left(\left(\mathbf{P}_1\right)^{T} \quad \left(\mathbf{P}_2\right)^{T} \quad \left(\mathbf{L}_1\right)^{T} \quad \left(\mathbf{L}_2\right)^{T}\right)^{T} \tag{6}$$

where $\mathbf{P}_i$ and $\mathbf{L}_i$ denote the DD pseudorange and carrier phase measurement vectors collecting all the relevant observables of the *p* DD SV pairs. VTECs above the receivers are modeled as two scalar first-order Gauss-Markov processes with equal correlation time scale, whereas cycle ambiguities are modeled as random constant plus random walk processes. The utilization of two VTECs and Lear's mapping function allows estimating all DD ionospheric delays as a function of only two variables: in this way the observability of the integer ambiguity by the reference solution is enhanced. Hence, the EKF non linear observation model *y=h(x)* can be written as

$$h(x)=\begin{pmatrix} I_p \\ I_p \\ I_p \\ I_p \end{pmatrix}\boldsymbol{\rho}(\mathbf{b}')+\begin{pmatrix} I_p \\ \gamma^{-2}I_p \\ -I_p \\ -\gamma^{-2}I_p \end{pmatrix}\mathbf{I}(\mathbf{VTEC})+\begin{pmatrix} 0_p \\ 0_p \\ 0_p \\ -\lambda_2 I_p \end{pmatrix}\mathbf{a}_w+\begin{pmatrix} 0_p \\ 0_p \\ \lambda_1 I_p \\ \lambda_2 I_p \end{pmatrix}\mathbf{a}_1 \tag{7}$$

where I_p is the p-dimensional identity matrix, **I** and **ρ** are the vectors of the DD ionospheric delays and signal paths for all the visible GPS satellite vehicles, respectively.

3.2 Wide-lane closed-loop EKF without ionospheric delays

The availability of dual-frequency GPS measurements makes it possible to form different measurement combinations that are able to remove completely the first-order ionospheric delay from the observation model, without the need of compensating it by estimation within the EKF state vector. In this section a formulation of the closed-loop EKF processing only such "iono-removed" measurements is presented. The state vector comprises thus only baseline, baseline rate, wide-lane, and L1 ambiguities, and its dynamics is governed by the same models of the previous sections.

$$x' \in \mathbb{R}^{(6+2p)\times 1},\ x'=\begin{pmatrix}\mathbf{b}' & \mathbf{a}_w & \mathbf{a}_1\end{pmatrix}^T \tag{8}$$

For obtaining an observation model without ionospheric delays, suitable combinations of DD measurements must be selected. GPS measurement combinations which allow for an exact cancellation of first-order ionospheric delays can be classified in three main families: ionospheric-free combinations [18], GRoup And PHase Ionospheric Corrections (GRAPHIC) [19], and Melbourne-Wubbena combinations [16]. The ionospheric-free combination (IF) is the most natural and diffuse combination for eliminating the ionospheric delay and it is based on combining observations of the same type on two carrier frequencies, exploiting the frequency dependence on the first-order ionospheric delay effect. With specific reference to the DD measurements reported in Eq.(3), two different ionospheric-free combinations can be derived, namely ionospheric-free combinations of pseudorange measurements and of carrier-phase measurements. GRAPHIC combinations exploit the asymmetry of the ionospheric effect on group and phase propagation at the same frequency. Again, two GRAPHIC combinations can be calculated considering L1 and L2 frequency, respectively. Finally, Melbourne-Wubbena combinations represent an estimate of WL ambiguities and cancel the ionospheric delays by combination of all four types of observables. These three families produce five types of combinations, which are not linearly independent.

Specifically, only three are linearly independent and therefore there is the need of selecting the three combinations the EKF has to process. With the aim of guaranteeing an accurate estimation of the baseline vector, but also a satisfactory observability of the entire state vector, ionospheric-free combination of carrier-phase measurements $\mathbf{L}_{IF}$, GRAPHIC combination on L1 frequency $\mathbf{G}_1$, and Melbourne-Wubbena combination **MW**, are selected, which can be derived from uncombined DD observables as follows

$$\mathbf{L}_{IF} = \frac{1}{1-\gamma^2}\left(\mathbf{L}_1 - \gamma^2 \mathbf{L}_2\right) \tag{9a}$$

$$\mathbf{G}_1 = 0.5\left(\mathbf{P}_1 + \mathbf{L}_1\right) \tag{9b}$$

$$\mathbf{MW} = \lambda_w\left(\frac{\mathbf{L}_1}{\lambda_1} - \frac{\mathbf{L}_2}{\lambda_2}\right) - \lambda_n\left(\frac{\mathbf{P}_1}{\lambda_1} + \frac{\mathbf{P}_2}{\lambda_2}\right) \tag{9c}$$

Combining the above definitions with the observation model in Eq.(3), the combined measurement vector y':=($\mathbf{L}_{IF}^T$, $\mathbf{G}_1^T$, $\mathbf{MW}^T$)^T can be related to the "iono-removed" state vector, y' = ,$h'(x')$ as follows

$$h'(x') = \begin{pmatrix} I_p \\ I_p \\ I_p \end{pmatrix} \boldsymbol{\rho}(\mathbf{b}') + \begin{pmatrix} \frac{\lambda_1 \gamma}{1-\gamma^2} I_p \\ 0_p \\ \lambda_w I_p \end{pmatrix} \mathbf{a}_w + \begin{pmatrix} \frac{\lambda_1}{1+\gamma} I_p \\ \frac{\lambda_1}{2} I_p \\ 0_n \end{pmatrix} \mathbf{a}_1 \tag{10}$$

4 Performance comparison on flight data

The performance of the two algorithms is evaluated on actual flight data made available by the Gravity Recovery and Climate Experiment (GRACE) mission, which consists of two identical satellites, GRACE A and GRACE B, in a leader-follower formation using near circular orbits [20]. Sensitivity to ionospheric conditions is evaluated by using datasets with different ionospheric activity levels. More precisely, two one-day long datasets have been chosen to represent the spectrum of possible ionospheric conditions. These range from mild, represented by DOY18, 2009, to intense, represented by DOY88, 2011. Discussion of how the ionospheric activity might be quantified for LEO applications is beyond the scope of this paper. Nonetheless, to put the difference between the datasets into perspective, the maximum VTEC recorded on Earth's surface can be treated as an indicator of the ionospheric activity. Whilst maximum VTEC values of 31 Total Electron Content Units (TECU) were recorded in DOY18, 2009, VTEC as high as 75 TECU were measured on ground on DOY88, 2011.

Both dataset comprise GPS L1B measurements at 0.1 Hz, Ka-Band Ranging System (KBR) data at 0.2 Hz , which allows estimating the true baseline at sub-millimeter accuracy, and GPS Navigation (GNV) L1B data at 1/60 Hz , which allows estimating

the three-dimensional baseline in ECEF. The KBR instrument measures the change in distance between the spacecraft, also known as the biased range, with a precision of 10 μm. The biased range can be seen as the true range plus an unknown bias. The bias is arbitrary for each piecewise continuous segment of phase change measurements and has to be compensated by a specially designed procedure, described in detail in [21]. The resulting accuracy is typically sub-millimetric because of the long time-spans over which data can be accumulated to compensate the unknown systematic bias. The Level 1B data includes also a GPS Navigation (GNV) data product, which contains an estimate of the two spacecraft Center of Mass (CoM) position and velocity vectors. These estimates are obtained as a product of a precision orbit determination tool [22] and typically have a time-varying accuracy of a few centimeters in each component. As with all GRACE Level 1B data, the time-tags are corrected to GPS time using GPS clock solutions computed in post-processing [22]. A data-editing step has been performed on GPS L1B data in order to detect and remove outliers in the pseudorange measurements and to discard all observations from GPS satellites whose elevation above the local horizon is smaller than 10 deg.

Estimation performance is quantified by comparing the baseline estimated by each filter to the reference solution obtained by KBR (for the magnitude) and GNV data (for the baseline vector components). Because of the different features of the data, the baseline magnitude estimation error can be quantified with very high accuracy, whereas estimation of the three-dimensional error is reliable only for error values at least in the order of 10 cm. Note that, due to GRACE mission's leader-follower formation, the baseline vector will be mostly directed along-track. Hence, KBR can be used also to estimate the along-track accuracy, whereas cross-track and radial accuracy will be corrupted by the worse precision of the reference GNV solutions. For providing additional insight into filters' performance, their capability of fixing the correct integer ambiguities is also analyzed. For this purpose, reference values of the integer ambiguities have been computed by exploiting the knowledge of the observation geometry provided by the KBR and GNV data. The adopted procedure is described in [10], to which we refer the interested reader.

The estimation performance of the two approaches is shown in Figure 3-Figure 6 and summarized in Table 1. More specifically, Figure 3 and Figure 4 show the time histories of the baseline magnitude estimation error and of the fixed integer ambiguities of the two approaches in mild ionospheric conditions. The baseline plot also highlights the time epochs in which the kinematic solution of the RTK algorithm in Figure 1 is not available, that is, when less than four WL ambiguities are fixed to integer values. The other two plots provide indications on the integer fixing performance of the filter, computed using the IA reference values. More specifically, at each time epoch a color-coded bar is shown, which stacks the number of IA estimated by LAMBDA that are correct or wrong. For a limited amount of IA, it has not been possible to determine the reference value, even with the knowledge of the true geometry by GRACE L1B data products. These are denoted as unknown IA. The potentially correct ambiguities given by LAMBDA can or cannot be fixed within the EKF, depending on the validation tests outcome. The number of IA fixed within the EKF is also shown.

It can be seen that both solutions have excellent WL fixing performance in mild ionospheric conditions. More than 90% of wide lane ambiguities are fixed in both cases with no errors. When using Lear's model, this has a beneficial effect also on the quality of the L1 LAMDA estimates, which, as shown in Figure 3, are mostly correct. Recall that only the L1 ambiguities that have a valid WL counterpart are fixed to the relevant integer value. Moreover, such L1 IA are used only for computing the kinematic

solution, but not for modifying the EKF estimate at later time instants (Figure 2). Therefore their number is denoted by a dashed line in all figures. The high WL ambiguity fixing rate allows computing the RTK solution in more than 90% of the time epochs in both approaches. However, the two solutions obtain L1 integer ambiguities solutions of different quality. Whilst using Lear's model allows for correct estimation of most L1 ambiguities (fail rate < 4%), the iono-removed solution fails to estimate the correct L1 ambiguity in more than 20% of the cases. These results suggest that removing the ionospheric delay model from the observation model decreases the correlation between WL and L1 ambiguities. Hence, correctly fixing the WL IA does not allow improving the L1 ambiguities estimates as in the previous case. This considerable amount of wrongly fixed ambiguities degrades the kinematic solution accuracy of the ionosphere-removed approach. Therefore, in mild ionospheric conditions, the degradation of the kinematic solution predominates over the benefits in the EKF baseline estimates that can be obtained from removing the ionospheric delay estimation error. As a result, the filter with Lear's model is capable of a RMS baseline magnitude estimation error smaller than 5 cm, less than half of the other approach.
Figure 5 and Figure 6 show the same results, but for intense ionospheric activity. As in DOY18, 2009, both solutions are still capable of correct WL IA estimation in more than 90% of the cases, and thus the RTK solution is almost always available. However, both filters fail almost one out of five L1 IA, with Lear's model still capable of better IA estimation than the ionosphere-removed solution. However, this fail rate results in a substantial increase of the baseline estimation error using Lear's model, whereas the no-ionosphere relative position solution does not degrade significantly w.r.t. mild ionospheric conditions. These results thus suggest that removing the ionospheric delay decreases not only the correlation between WL and L1 ambiguities, but also the one between the L1 ambiguities and the baseline, probably because of the worse observability of the unknowns. As a consequence, the iono-removed approach as a performance less sensitive to the ionospheric delays magnitude than the one using Lear's model. In intense ionospheric conditions, the former is thus capable of better positioning performances.

5 Conclusion

This paper has focused on CDGPS-based real-time onboard relative positioning of two LEO GPS receivers separated by hundreds of kilometers. Compensation of the double-difference ionospheric delays is known to be one of the limiting factors in relative positioning over large baselines. Different approaches have been analyzed for compensating ionospheric delays in such applications, and two of them have been developed in detail. While the first one attempts to predict all double-difference ionospheric delays by knowledge of the vertical total electron content above the two receivers, the second solution deletes all first order ionospheric delays from the problem by proper combination of GPS observables.
Effectiveness of the two approaches has been evaluated on actual flight data from the GRACE mission. To this end, the accuracy in predicting both the receivers' relative position and the double difference carrier-phase cycle ambiguities has been evaluated using a previously developed positioning approach. As the ionospheric effects heavily depend on the status of the ionosphere, the comparison has been made on two

different datasets, chosen to represent the possible spectrum of ionospheric conditions.
Results show that ionospheric activity plays a major role in determining the relative positioning performance. While the relative positioning performance degrades as the ionosphere's electron content increase when modeling the ionosphere, positioning without predicting ionospheric delays is faintly sensitive to ionospheric activity. As a result, modeling the delays is advantageous for relative positioning in mild ionospheric conditions. As the ionosphere's electron content increases, this approach becomes less capable of accurate relative positioning, and the solution without ionospheric delays becomes preferable.
In addition, results suggest that removing the ionospheric delays from the observation model decreases the correlation between WL and L1 ambiguities, and between the ambiguities and the baseline. In fact, while its relative position solution is relatively insensitive to the ionospheric activity, the ambiguity solution is always worse than the one obtained modeling the ionospheric delays.

References

[1] R. Kroes, O. Montenbruck, W. Bertiger, P. Visser, Precise GRACE baseline determination using GPS, GPS Solutions, Volume 9, Issue 1, pp 21-31, April 2005.

[2] U. Tancredi, A. Renga, M. Grassi, Carrier-based Differential GPS for autonomous relative navigation in LEO, AIAA Guidance Navigation and Control Conference, August 2012, 11 pp., paper id AIAA-2012-4707.

[3] Montenbruck O. et all, Carrier Phase Differential GPS for LEO Formation Flying - The PRISMA and TanDEM-X Flight Experience, Astr.Sp.Conf, 2011

[4] D'Amico, S., Ardaens, J. S., and Larsson, R. Spaceborne Autonomous Formation-Flying Experiment on the PRISMA Mission, Journal of Guidance Control and Dynamics Vol.35 no.3, 2012. pp.834-850.

[5] S. Leung, O. Montenbruck, Real-Time Navigation of Formation-Flying Spacecraft Using Global-Positioning-System Measurements, Journal Of Guidance, Control, And Dynamics, Vol. 28, No. 2, March–April 2005, pp. 226-235.

[6] Ebinuma, T., Bishop, R.H. and Glenn Lightsey, E. Integrated hardware investigations of precision spacecraft rendezvous using the global positioning system, Journal of Guidance Control and Dynamics 26, no. 3, 2003. pp. 425-433.

[7] S.-Ch.Wu, Y.E. Bar-Sever, Real-time sub-cm differential orbit determination of two Low-Earth Orbiters with GPS bias fixing; ION GNSS 2006; September 26-29, 2006 Fort Worth, Texas, 2006.

[8] W.M. Lear, GPS navigation for low-earth orbiting vehicles, NASA Lyndon B. Johnson Space Center, Mission planning and analysis division, 1st revision, NASA 87-FM-2, JSC-32,031, 1988.

[9] U. Tancredi, A. Renga, M. Grassi, Validation on flight data of a closed-loop approach for GPS-based relative navigation of LEO satellites, Acta Astronautica Vol. 86, pp. 126-135, 2013.

[10] U. Tancredi, A. Renga, M. Grassi, “Ionospheric path delay models for spaceborne GPS receivers flying in formation with large baselines”, Advances in Space Research, Vol. 48, No. 3, pp. 507–520, August 2011.

[11] Tancredi, U., Renga A., and Grassi, M. “Real-Time Relative Positioning of Spacecraft over Long Baselines”, Journal of Guidance, Control, and Dynamics, *in print*

[12] Tancredi U., Renga, A., and Grassi, M., “GPS-Based Relative Navigation of LEO Formations with Varying Baselines,” AIAA Guidance, Navigation, and Control Conference, Toronto, Canada, August 2010.

[13] Teunissen PJG (1995), The least-squares ambiguity decorrelation adjustment: a method for fast GPS integer ambiguity estimation. Journal of Geodesy, Vol.70, pp. 65-82.

[14] S. Verhagen, The GNSS integer ambiguities: estimation and validation, Ph.D. Thesis, Delft TU, 2005.

[15] Teunissen P, Verhagen S (2007) GNSS carrier phase ambiguity resolution: challenges and open problems. In: Proceedings of the scientific meetings of the IAG general assembly 2007. Perugia, Italy.

[16] Melbourne, W.G. (1985), The case for ranging in GPS-based geodetic systems, in Proceedings of the 1st Intenational Symposium on Precise positioning with the Global Positioning System, pp. 373–386, Rockville, Maryland.

[17] Teunissen, P.J.G. On the GPS widelane and its decorrelating property, Journal of Geodesy, 1997, Volume 71, Issue 9, pp 577-587

[18] J. Farrel , M. Barth, The Global Positioning System and Inertial Navigation, McGraw-Hill, New York, ch. 5, 1999.

[19] Yunck, T. P. Orbit determination, in: Parkinson B.W., Spilker, J.J. (eds), Global positioning system: theory and applications, vol. 2, American Institute of Aeronautics and Astronautics Inc., Washington, pp. 559-592, 1996

[20] Tapley, B. D., Bettadpur, S., Watkins, M., Reigber, C. The gravity recovery and climate experiment mission overview and early results, Geophys. Res. Lett., 31, L09607, 2004.

[21] Kroes, R. Precise relative positioning of formation flying spacecraft using GPS, Ph.D. thesis, Delft University of Technology, The Netherlands, 2006.

[22] Case, K., Kruizinga, G., Wu, S.C. GRACE level 1B data product user handbook, NASA Jet Propulsion Laboratory, revision 1.3, JPL D-22027, GRACE 327-733, 2010.

FIGURES AND TABLES

Figure 1. Schematic representation of the reference relative positioning approach

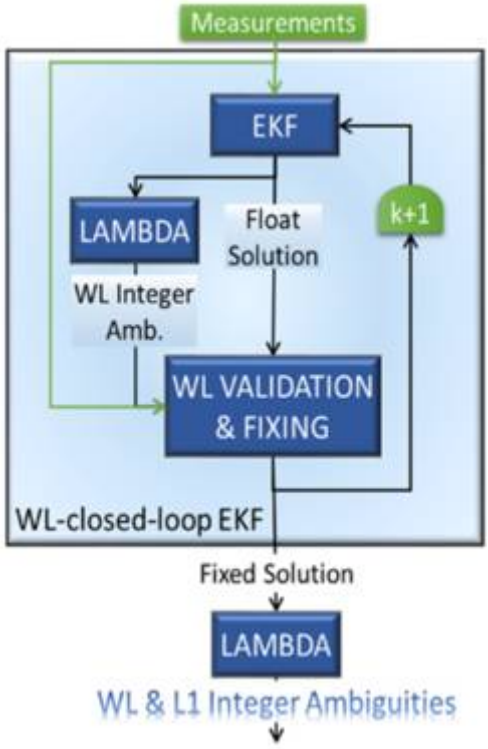

Figure 2. OTF ambiguity resolution flow diagram.

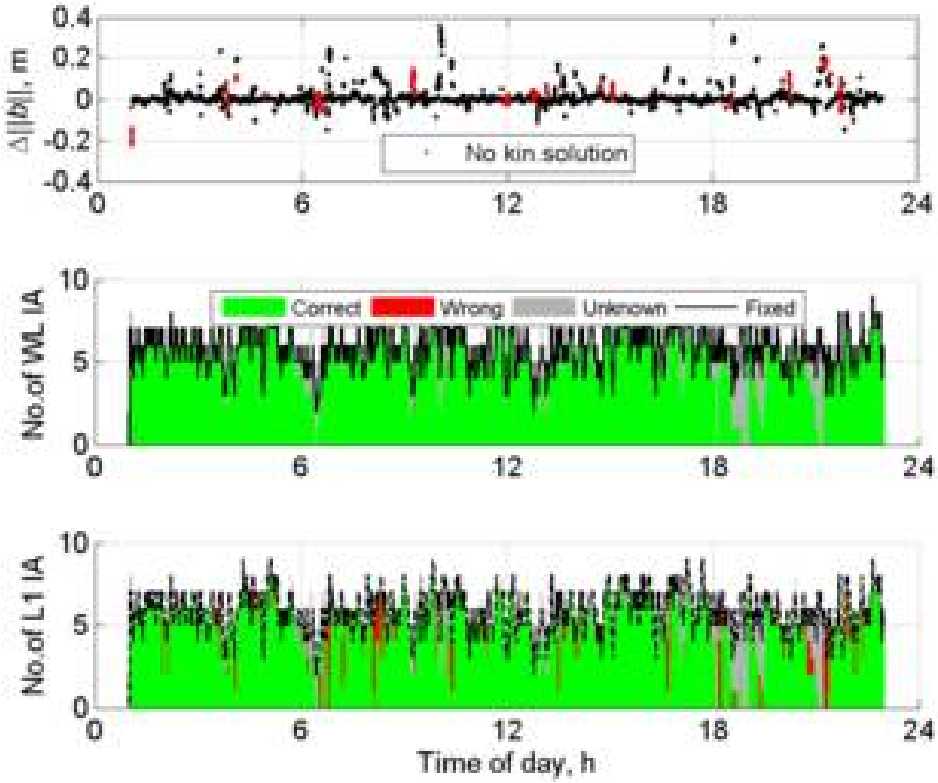

Figure 3. Performances using Lear's model in DOY18,09: baseline norm estimation error (top), WL (middle) and L1 (bottom) IA fixing.

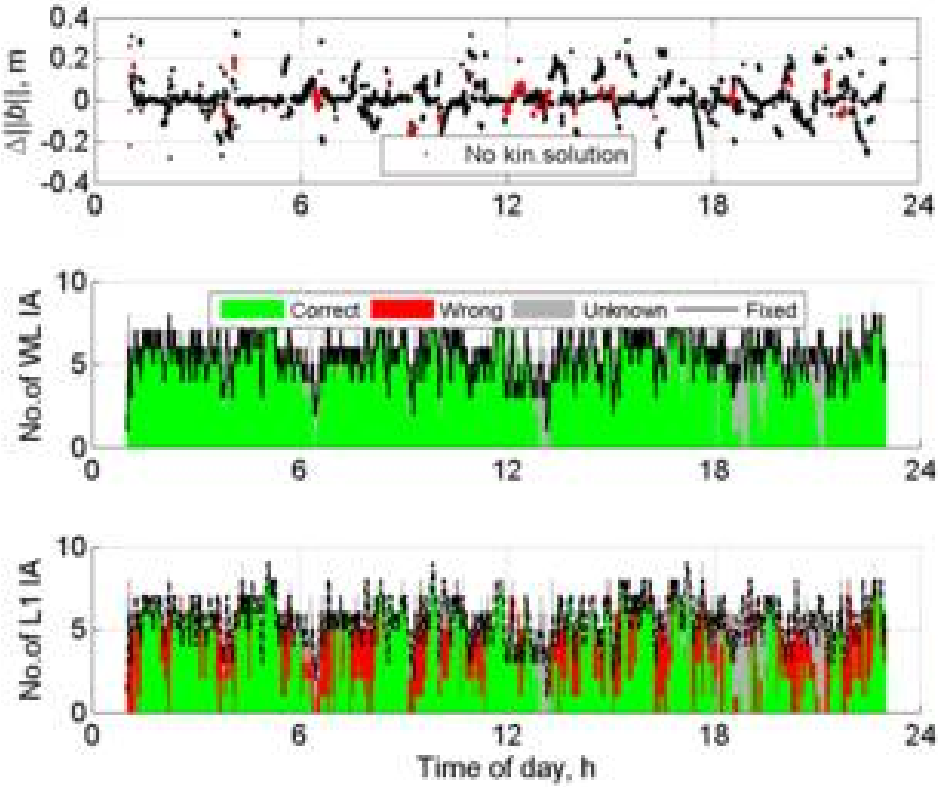

Figure 4. Performances without ionospheric delays in DOY18,09: baseline norm estimation error (top), WL (middle) and L1 (bottom) IA fixing.

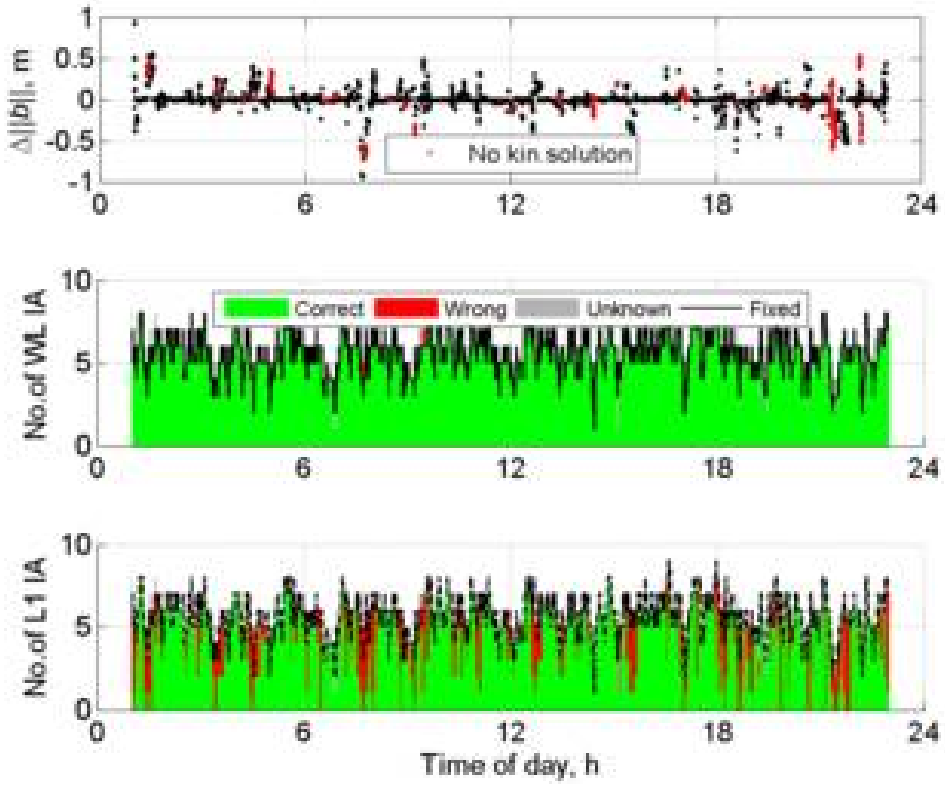

Figure 5. Performances using Lear's model in DOY88,11: baseline norm estimation error (top), WL (middle) and L1 (bottom) IA fixing.

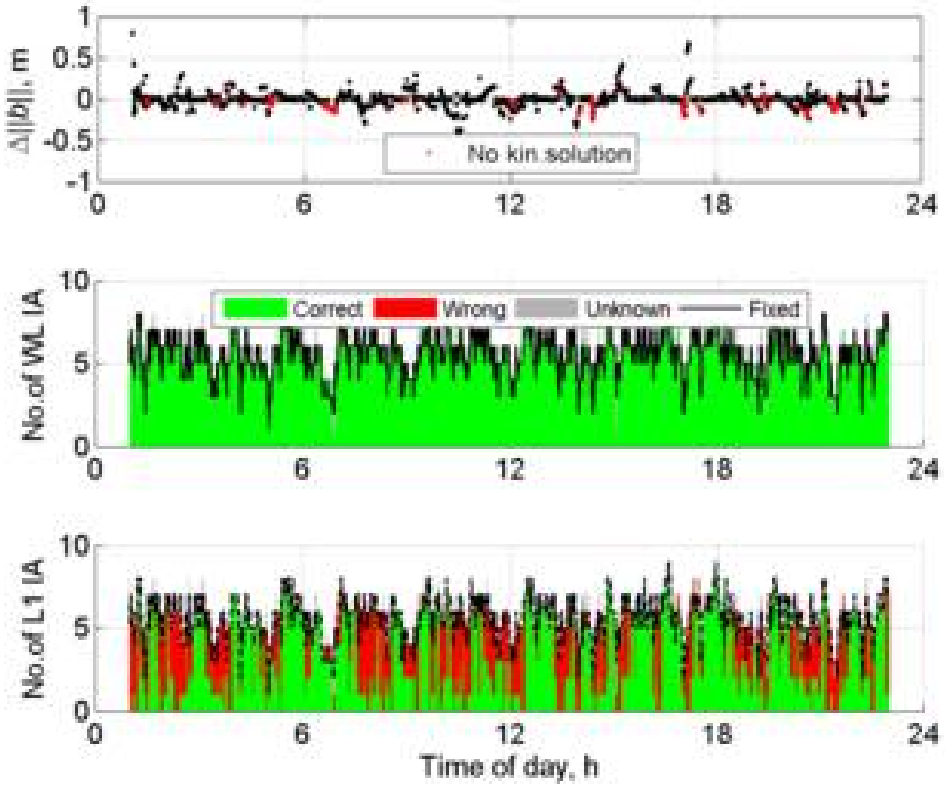

Figure 6. Performances without ionospheric delays in DOY88,11: baseline norm estimation error (top), WL (middle) and L1 (bottom) IA fixing.

Table 1.Estimation Performance Summary

	Lear's model				Ionosphere removed			
	DOY18,09		*DOY88,11*		*DOY18,09*		*DOY88,11*	
Baseline Component	**Baseline estimation error, cm**							
	max / RMS		*max / RMS*		*max / RMS*		*max / RMS*	
Magnitude (||b||)	35.8	4.2	105.0	12.2	85.5	8.6	80.6	9.3
Along Track (b_x)	36.9	4.5	105.0	12.1	110.0	8.9	84.1	9.3
Cross Track (b_y)	28.0	2.4	36.4	2.8	35.3	7.7	132.8	10.0
Radial (b_z)	91.2	6.8	297.1	15.3	70.3	8.8	95.6	10.4
RTK Availability	96.3%		94.5%		93.5%		92.6%	
Ambiguity	**Integer ambiguites estimation rates, %**							
	Fixing	*Fail*	*Fixing*	*Fail*	*Fixing*	*Fail*	*Fixing*	*Fail*
WL ambiguities	98.0	0.0	97.0	0.0	93.4	0.0	95.2	0.1
L1 ambiguities	98.0	3.6	97.0	11.2	93.4	21.2	95.2	26.4